SUPPORTING INFORMATION

High Open-Circuit Voltage Roll-to-Roll Compatible Processed Organic Photovoltaics

Francesco Tintori, Audrey Laventure, Josh D. B. Koenig and Gregory C. Welch*

Department of Chemistry, University of Calgary, 2500 University Drive N.W., Calgary, AB, Canada, T2N 1N4

*gregory.welch@ucalgary.ca

Table of contents

Materials and Methods

Materials: PTQ10 purchased from *Brilliant Matters* and utilized without further purification. $tPDI_2N$-EH was synthetized in our laboratories following published procedures from our group.[1] PDI-EDOT-PDI was synthesized following the procedure reported herein, with all synthetic and characterization details available below (p. S16-S18)

Solution Preparation:

PTQ10:$tPDI_2N$-EH solutions were prepared in air, from 10 mg/mL solutions of the single components, which were stirred for 2 h before mixing in the required weight proportions. If applicable, diphenyl ether (DPE) was added to the solution in the desired v/v proportion. Final solutions were stirred for at least 1 h before deposition.

ZnO precursor solutions were prepared following the sol-gel method proposed by Sun et al.[2], 1 g of zinc acetate trihydrate, 0.280 mL of ethanolamine and 10.0 mL of 2-methoxy ethanol were mixed in air and stirred overnight at room temperature before use.

Film Preparation: All studied films were prepared as follow: pre patterned ITO-coated glass substrates (15x15 mm) were first cleaned by surfactant/water scrubbing, followed by sequentially ultra-sonicating in de-ionized water, acetone and isopropanol (10+ minutes each) before use. ITO substrates were then dried with pressurized air and UV-Ozone treated for 30 minutes. A ZnO precursor solution was spin-coated onto the ITO substrate at a speed of 4500 rpm for 60 s and then thermally annealed at 200 °C for 30 min. The organic layer was then cast at room temperature, in air, by either spin-coating at 1000 rpm for 60 s or coated using a 13 mm slot-die head (FOM Technologies Sheet Coater), at room temperature and at a rate of 40 cm/min (0.5 cm/s) with an automated dispensing solution source set at 80 µL/min (1.25 µL/s). Slot-die coating was carried out over 5-10 aligned glass/ITO slides, producing a 10-15 cm long slot-die coated film.

Optical Absorption Spectroscopy (UV/vis/near-IR): All absorption measurements were recorded using an Agilent Technologies Cary 60 UV-vis spectrometer at room temperature.

Optical Photoluminescence Spectroscopy: All measurements were recorded using an Agilent Technologies Cary Eclipse fluorescence spectrophotometer at room temperature.

Atomic Force Microscopy (AFM): AFM measurements were performed by using a TT-2 AFM (AFM Workshop, USA) in the tapping mode and WSxM software with a 0.01-0.025 Ohm/cm Sb (n) doped Si probe with a reflective back side aluminum coating.

Photovoltaic Cells Fabrication: All cells were fabricated following the initial procedure for cleaning, ZnO deposition and organic layer deposition reported above. The fabricated films were then moved to an N_2 atmosphere glovebox for 24 h before evaporating MoO_x and Ag. 10 nm of MoO_x followed by 100 nm of Ag were thermally deposited under high vacuum (10^{-5} torr) as determined by a shadow mask, producing contacts of 14 mm^2 (rectangular shaped, 7x2 mm).

Photovoltaic Cells Testing: One sun testing: current density-voltage (J-V) characteristics were measured using a Keithley 2420 Source Measure Unit. Solar cell performance used an Air Mass 1.5 Global (AM 1.5G) Solar Simulator (Newport, Model 92251A-1000) with an irradiation intensity of 100 mW/cm^2, which was measured by a calibrated silicon solar cell and a readout meter (Newport, Model 91150V). External Quantum Efficiency (EQE): EQE was measured in a QEX7 Solar Cell Spectral Response/QE/IPCE Measurement System (PV Measurement, Model QEX7, USA) with an optical lens to focus the light into an area about 0.04 cm, smaller than the dot cell. The silicon photodiode was used to calibrate the EQE measurement system in the wavelength range from 300 to 1100 nm. Low-light conditions determination and testing are described in pages S10-S13.

Nuclear Magnetic Resonance (NMR): ^{1}H and ^{13}C NMR spectroscopy experiments were recorded using either a Bruker Avance III 500 MHz spectrometer. All experiments were performed in chloroform-d ($CDCl_3$). Chemical shifts (referenced to residual solvent) were reported in parts per million (ppm).

High-resolution MALDI-TOF (HR MALDI-TOF): High-resolution MALDI-TOF mass spectrometry measurements were performed courtesy of Jian Jun (Johnson) Li in the Chemical Instrumentation Facility at the University of Calgary. The sample solution (~ 1 µg/ml in dichloromethane) was mixed with matrix trans2-[3-(4-tert-Butylphenyl)-2-methyl-2-propenylidene]malononitrile (DCTB) solution (~5 mg/ml in methanol). All spectra were acquired using a Bruker Autoflex III Smartbeam MALDI-TOF, set to the positive reflective mode (Na:YAG 355 nm laser settings: laser offset = 62-69; laser frequency = 200Hz; and number of shots = 300). The target used was Bruker MTP 384 ground steel plate target.

Cyclic Voltammetry (CV): Electrochemical measurements were performed using a CH Instruments Inc. Model 1200B Series Handheld Potentiostat. A standard 3-electrode setup was utilized, consisting of a freshly polished glassy carbon disk working electrode (WE), Pt-wire counter electrode (CE), and Ag-wire pseudo-reference electrode (RE). All measurements were referenced to ferrocene ($Fc^{+/0}$) as internal standard. All cyclic voltammetry experiments were performed at a scan rate of 100 mV/s. Sample solutions, with 1 mM compound and 0.1 M tetrabutylammonium hexafluorophosphate ($TBAPF_6$) supporting electrolyte, were prepared in anhydrous CH_2Cl_2. All electrochemical solutions were sparged with dry gas (either N_2 or argon) for 5 minutes to deoxygenate the system prior to measurements. The ionization potentials (IP) and electron affinities (EA) were estimated by correlating the onsets (E_{ox} $Fc^{0/+}$, E_{red} $Fc^{0/+}$) to the normal hydrogen electrode (NHE), assuming the IP of $Fc^{0/+}$ to be 4.80 eV.[3]

OPV Devices: Investigation of DPE Processing Additive

These experiments were carried out to probe the effect of the solvent additive diphenyl ether (DPE) on the system performance when using different non-halogenated solvents and different solvent additive loads. The goal was to demonstrate the viability of this system with a variety of non-halogenated solvents and the consistency of the behaviour with the solvent additive. Solvent additive loads (v/v %) from 0.25 to 3 % were tested with toluene, *o*-xylene and 1,2,4-trimethylbenzene (TMB) and it was found that in all cases a DPE load of 1% resulted in the best device performance.

This effect was then further explored by looking at changes in the optical properties of the BHJ blend (absorption via UV-Vis spectroscopy and emission via PL spectroscopy, Figure S2). The optical absorption shows the growing of the 600 nm band, which was previously reported by our group, and is believed to correspond with the PDI molecular acceptor self assembly. This is believed to provide a more favorable morphology, which in turns results in a higher fill factor and photocurrent. PL spectroscopy shows complete quenching of the polymer emission, which proves the existence of efficient charge transfer from donor to acceptor.

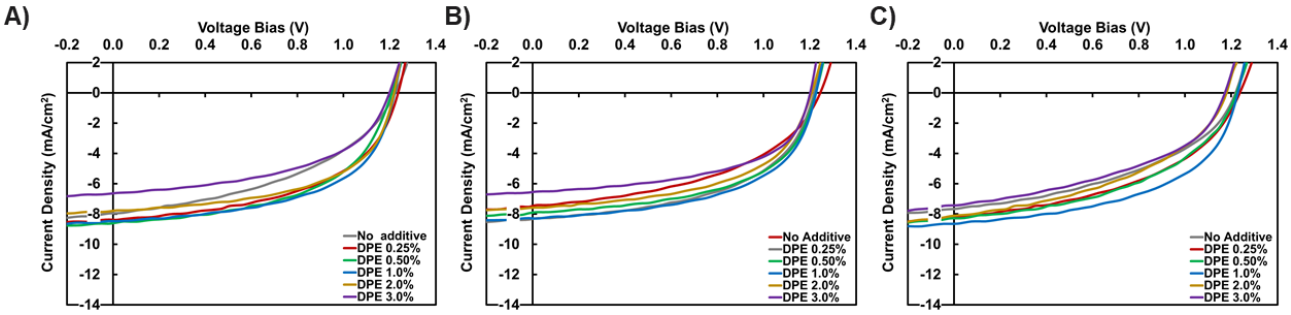

Figure S1. Current density – voltage (J-V) curves of OPV devices with PTQ10:tPDI$_2$N-EH active layer processed from A) toluene, B) *o*-xylene or C) TMB with various amounts of DPE solvent processing additive (0-3% (v/v)).

Table S1. OPV parameters of devices with PTQ10:tPDI$_2$N-EH active layers processed from toluene, *o*-xylene or TMB with various amounts of DPE solvent processing additive (0-3% (v/v)) under one sun illumination (AM 1.5).

		V_{oc} (V)			J_{sc} (mA/cm^2)			FF %			PCE %		
Toluene	No Additive	1.22	±0.01	(1.23)	7.6	±0.25	(7.8)	44	±1	(45)	4.0	±0.1	(4.3)
	DPE 0.25%	1.23	±0.01	(1.23)	8.2	±0.11	(8.3)	50	±1	(52)	5.0	±0.2	(5.3)
	DPE 0.50%	1.20	±0.01	(1.21)	8.3	±0.28	(8.6)	53	±1	(53)	5.3	±0.2	(5.5)
	DPE 1.0%	1.21	±0.01	(1.22)	8.2	±0.25	(8.5)	55	±1	(56)	5.5	±0.2	(5.8)
	DPE 2.0%	1.21	±0.02	(1.22)	7.7	±0.42	(7.8)	54	±2	(56)	5.1	±0.3	(5.3)
	DPE 3.0	1.17	±0.00	(1.20)	6.4	±0.20	(6.6)	48	±1	(50)	3.6	±0.1	(4.0)
o-Xylene	No Additive	1.24	±0.00	(1.24)	7.4	±0.19	(7.5)	45	±1	(47)	4.2	±0.2	(4.4)
	DPE 0.25%	1.22	±0.01	(1.22)	8.0	±0.20	(8.3)	50	±2	(53)	4.9	±0.3	(5.4)
	DPE 0.50%	1.21	±0.01	(1.21)	7.9	±0.14	(8.0)	52	±3	(53)	4.9	±0.3	(5.2)
	DPE 1.0%	1.22	±0.01	(1.22)	8.0	±0.18	(8.3)	54	±1	(55)	5.3	±0.2	(5.6)
	DPE 2.0%	1.20	±0.02	(1.22)	7.7	±0.23	(8.2)	51	±5	(55)	4.7	±0.6	(5.5)
	DPE 3.0	1.20	±0.00	(1.20)	6.5	±0.03	(6.5)	55	±0	(55)	4.3	±0.0	(4.3)
TMB	No Additive	1.20	±0.00	(1.20)	7.5	±0.07	(7.4)	42	±1	(44)	3.8	±0.1	(3.9)
	DPE 0.25%	1.21	±0.01	(1.22)	8.1	±0.22	(8.3)	45	±1	(47)	4.4	±0.2	(4.8)
	DPE 0.50%	1.23	±0.01	(1.23)	8.2	±0.04	(8.1)	46	±1	(47)	4.6	±0.1	(4.7)
	DPE 1.0%	1.21	±0.01	(1.23)	8.3	±0.23	(8.6)	50	±2	(52)	5.0	±0.3	(5.5)
	DPE 2.0%	1.18	±0.00	(1.18)	7.9	±0.14	(7.9)	45	±1	(47)	4.2	±0.1	(4.4)
	DPE 3.0	1.18	±0.01	(1.17)	7.5	±0.35	(8.1)	42	±2	(41)	3.7	±0.3	(3.9)

* values are a calculated average over 8 or more devices
** device architecture used: glass/ITO/ZnO/Active Layer BHJ/MoO_x/Ag
***values in brackets represent the best device

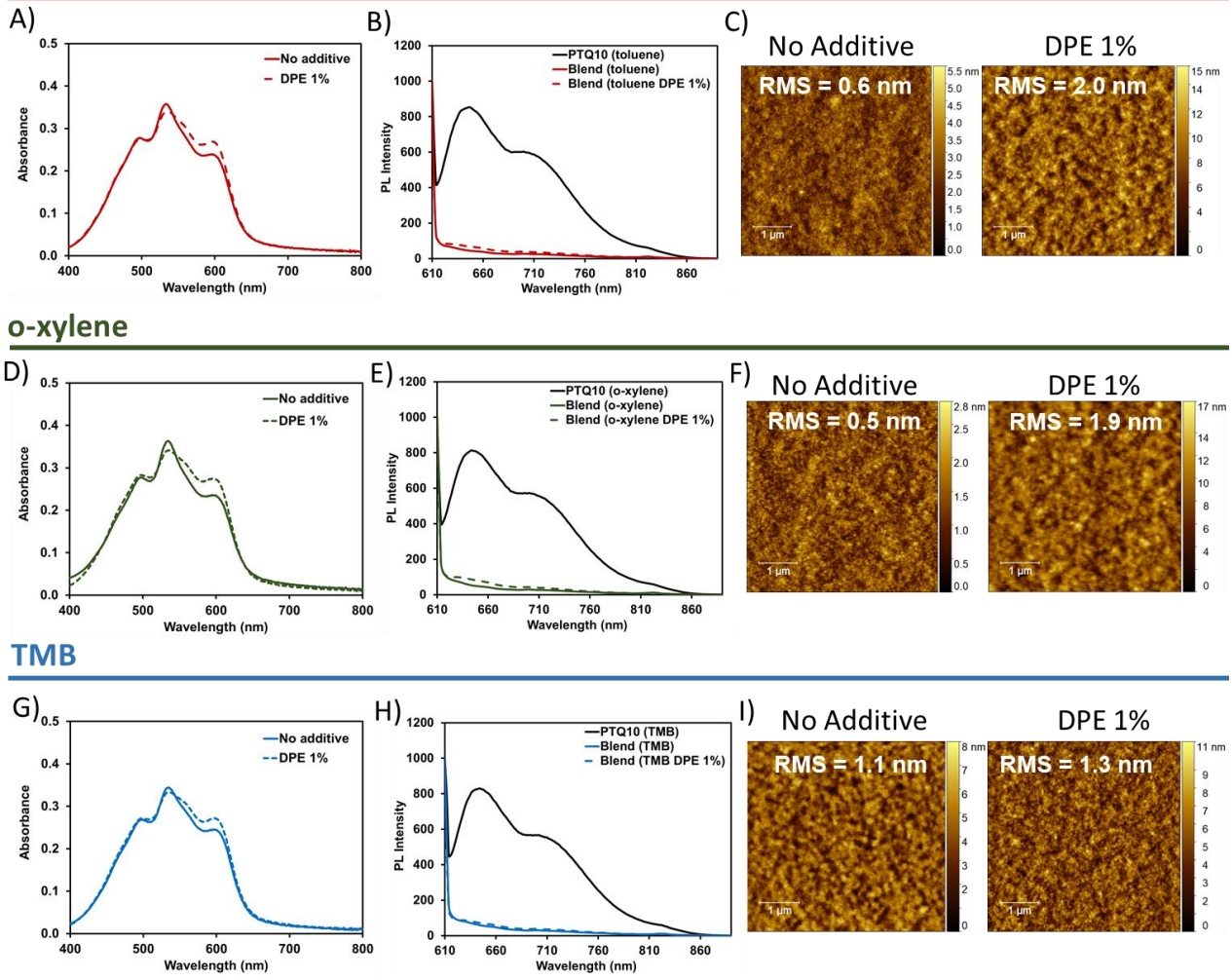

Figure S2. A,D,G) Optical absorption profiles, B,E,H) photoluminescence emission profiles, and C,F,I) atomic force microscopy (AFM) height images with corresponding root mean square roughness (RMS)of PTQ10:tPDI$_2$N-EH films processed from toluene, *o*-xylene or TMB with or without 1% (v/v) DPE.

OPV Devices: Slot-Die Coating Active Layer.

Figure S3. Pictures of PTQ10:tPDI$_2$N-EH films fabricated by spin-coating (left) and slot-die coating (right).

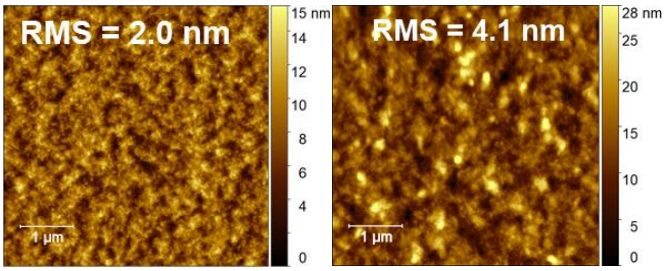

Figure S4. AFM height images with corresponding RMS value of the spin-coated (left) and the slot-die coated (right) films of PTQ10:tPDI$_2$N-EH BHJ blends processed from toluene with 1% (v/v) DPE.

OPV Devices: Interlayer and Third-Component

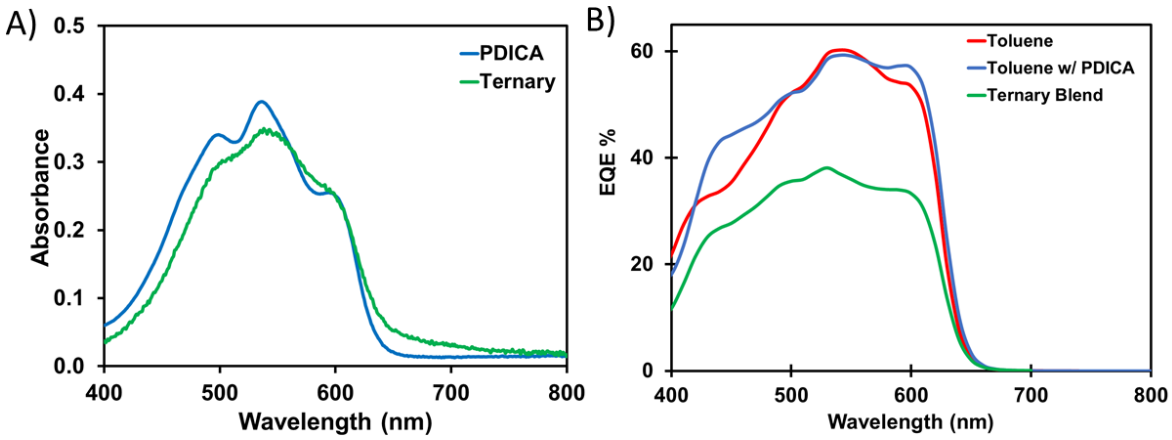

Figure S5. A) Optical absorption profiles of PTQ10:tPDI$_2$N-EH active layers cast on top of ITO/ZnO/ PDICA and PTQ10:tPDI$_2$N-EH:PDI-EDOT-PDI (1:0.8:0.2) BHJ blends cast on top of ITO/ZnO processed from toluene/DPE 1% (v/v). B) EQE profiles of OPV devices with PTQ10:tPDI$_2$N-EH active layers cast on top of ITO/ZnO or ITO/ZnO/PDICA and PTQ10:tPDI$_2$N-EH:PDI-EDOT-PDI (1:0.8:0.2) BHJ blends cast on top of ITO/ZnO processed from toluene/DPE 1% (v/v).

Table S2. OPV parameters of devices with PTQ10:PDI-EDOT-PDI BHJ active layer blends processed from *o*-xylene under one sun illumination (AM 1.5).

	V_{oc} (V)			J_{sc} (mA/cm^2)			FF %			PCE %		
No additive	1.29	±0.01	(1.32)	2.5	±0.06	(2.53)	26	±0	(26)	0.8	±0.0	(0.9)
DPE 1%	1.32	±0.01	(1.34)	4.0	±0.06	(4.12)	33	±0	(34)	1.8	±0.1	(1.9)

* values are a calculated average over 8 or more devices
** device architecture used: glass/ITO/ZnO/Active Layer BHJ/MoO_x/Ag
***values in brackets represent the best device

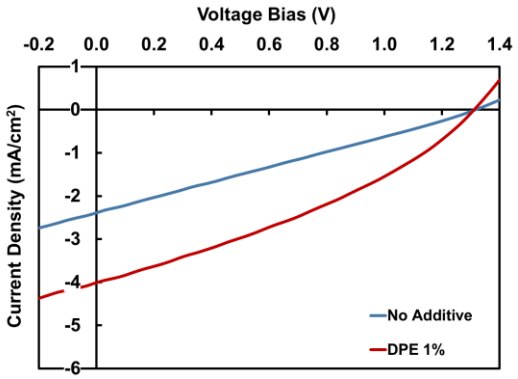

Figure S6. Current density – voltage curves of devices with PTQ10:PDI-EDOT-PDI active layers processed from *o*-xylene under one sun illumination (AM 1.5)

OPV Devices: testing under LED illumination

LED source and irradiance profile: A Coidak LED light bulb was used as the LED illumination source. Its spectral irradiance profile was recorded using an Ocean Insight Flame-S-Vis-NIR-ES spectrometer connected to a FOIS-1 integrating sphere using a 2 m long, 400 um Vis/NIR optic fiber.

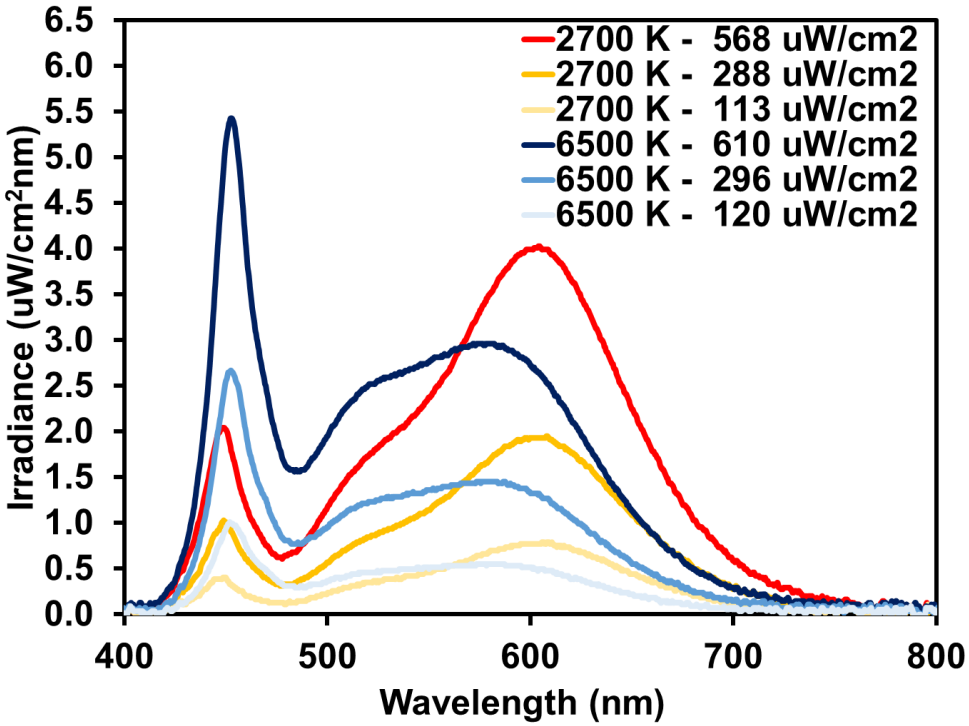

Figure S7. Emission spectra (irradiance profiles) of the LED light bulb set at various illumination conditions.

Power input (P_{in}) measurements and calculations: The P_{in} was measured using a Newport Si-photodiode (818-SL/DB, 1 cm^2 area) connected to an Ossila XTralien X200 source measure unit. The Si-photodiode was positioned at three different distance from the LED light bulb, corresponding to the three distances at which the OPV devices were positioned upon their testing. The current produced by the Si-photodiode were recorded at both 2700 K and 6500 K LED illumination, as exemplified in Figure S7A.

*All devices were light soaked under the solar simulator halogen lamp for 10 s before testing under LED light. This was necessary to allow conduction in the ZnO cathodic interlayer as previously reported in literature. [4–8]

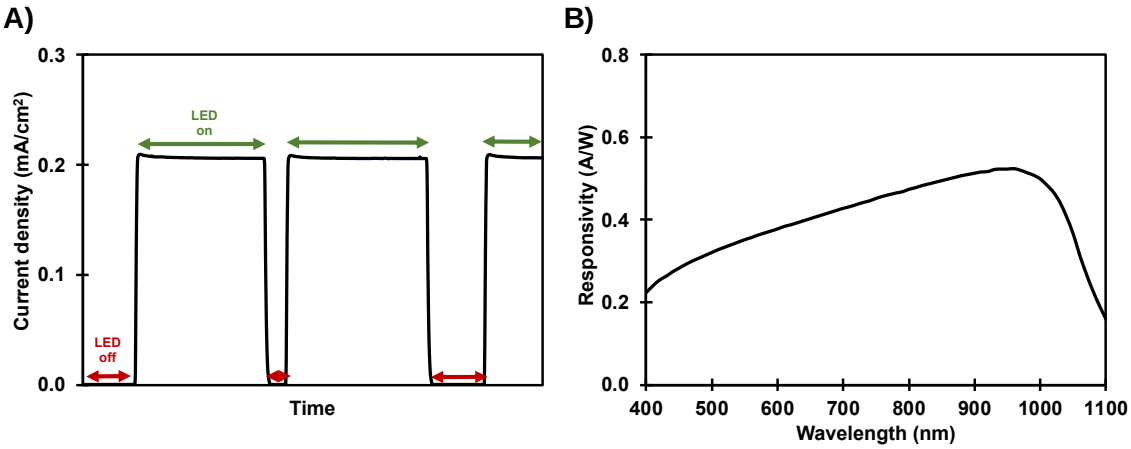

Figure S8. Si-photodiode A) current density response under a 2700 K LED illumination (distance A, ca. 2000 lux) and B) responsivity.

Table S3. Current density response ($J_{measured}$, mA/cm^2) of the Si-photodiode under the different LED illumination used for the OPV testing.

	$J_{measured}$ at Distance A (mA/cm^2)	**$J_{measured}$ at Distance B** (mA/cm^2)	**$J_{measured}$ at Distance C** (mA/cm^2)
2700 K	0.208	0.105	0.041
6500 K	0.209	0.101	0.041

The P_{in} was then calculated using Equation S1.[9]

$$P_{in} = K \times \int \Phi_{LED,\,normalized} = \frac{J_{measured}}{J_{calculated}} \times \int \Phi_{normalized} = \frac{J_{measured}}{\int \Phi_{LED,\,normalized} \times R_{photodiode}} \times \int \Phi_{LED,\,normalized}$$

Equation S1

Where $J_{measured}$ corresponds to the current density response of the Si-photodiode (values reported in Table S3); Φ_{LED} is the irradiance spectra of the LED (Figure S6) and $R_{photodiode}$ (Figure S7B) is the responsivity of the Si-photodiode.

The calculated P_{in} values are reported in Table S4.

Table S4. P_{in} values (in $\mu W/cm^2$) calculated according to Equation S1.

	Distance A	**Distance B**	**Distance C**
2700 K	568	288	113
6500 K	610	294	120

Illuminance measurements and calculations. The illuminance (*I*) measurements were measured using a commercial digital luxmeter (Dr Meter). The values are reported in Table S5. The illuminance at which the OPV devices were tested can also be calculated using the Si-photodiode response, according to Equation S2 and considering that the lm/m^2 unit corresponds to the lux unit.[9]

$$I = 683\ \frac{lm}{W} \times \mathrm{K} \times \int \Phi_{\mathrm{LED,\ normalized\ @\ 555\ nm}} \times V \qquad \textbf{Equation S2}$$

$$= 683\ \frac{lm}{W} \times \frac{J_{measured}}{J_{calculated}} \times \int \Phi_{LED,normalized\ @\ 555\ nm} \times V$$

$$= 683\ \frac{lm}{W} \times \frac{\mathrm{J_{measured}}}{\int \Phi_{\mathrm{LED,\ normalized}} \times \mathrm{R_{photodiode}}} \times \int \Phi_{\mathrm{LED,\ normalized\ @\ 555\ nm}} \times V$$

Where *I* corresponds to the illuminance values and *V* is the photopic response (Figure S8). Since the photopic response function has a maximum at 555 nm, the 683 lm/W factor is used at the luminous efficiency and could be responsible of the discrepancy between the $I_{measured}$ and $I_{calculated}$ that are reported in Table S5.

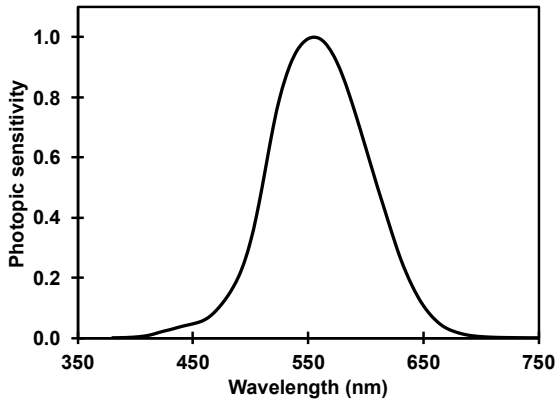

Figure S9. Photopic response function.

Table S5. Illuminance values ($I_{measured}$ using a digital luxmeter and $I_{calculated}$ according to Equation S2) reported in lux.

	Distance A	**Distance B**	**Distance C**
2700 K			
$I_{measured}$	1750-1800	870-900	350-380
$I_{calculated}$	1410	714	282
6500 K			
$I_{measured}$	1900-1950	930-970	380-400
$I_{calculated}$	1230	597	243

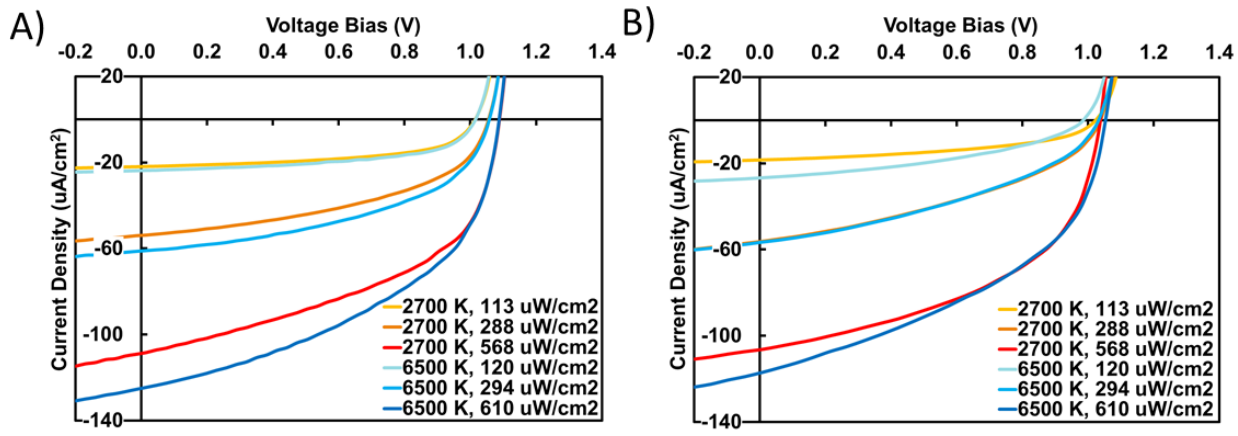

Figure S10. Current density – voltage curves of devices with PTQ10:tPDI$_2$N-EH active layers processed from toluene/DPE 1% (v/v) spin-coated on top of A) ITO/ZnO or B) ITO/ZnO/PDICA (B) under various LED illumination conditions

Table S6. OPV parameters of PTQ10:tPDI$_2$N-EH (Slot-die coated and spin-coated on top of PDICA interlayer) and PTQ10:tPDI$_2$N-EH:PDI-EDOT-PDI (1:0.8:0.2) ternary blend films

		V_{oc} (V)	J_{sc} (mA/cm^2)	FF %	PCE %
Slot-Die Coated		1.20 ±0.01 (1.20)	8.0 ±0.5 (8.9)	52 ±2 (50)	5.0 ±0.2 (5.4)
Interlayer		1.24 ±0.00 (1.24)	8.9 ±0.2 (9.2)	55 ±1 (56)	6.1 ±0.2 (6.4)
Ternary		1.24 ±0.01 (1.25)	7.7 ±0.2 (8.2)	40 ±1 (40)	3.8 ±0.1 (4.1)
		V_{oc} (V)	J_{sc} (µA/cm^2)	FF %	PCE %
Slot-Die Coated	2700 K	1.07 ±0.01 (1.06)	105 ±4 (110)	51 ±1 (53)	10.1 ±0.5 (10.9)
	6500 K	1.08 ±0.01 (1.08)	118 ±1 (118)	50 ±1 (52)	10.4 ±0.2 (11.6)
Interlayer	2700 K	1.09 ±0.01 (1.10)	112 ±3 (116)	51 ±4 (58)	10.9 ±1.1 (12.9)
	6500 K	1.07 ±0.01 (1.06)	139 ±9 (152)	48 ±3 (47)	11.7 ±0.4 (12.4)
Ternary	2700 K	1.10 ±0.00 (1.10)	101 ±1 (102)	48 ±1 (48)	9.2 ±0.3 (9.5)
	6500 K	1.11 ±0.01 (1.11)	116 ±2 (116)	47 ±1 (48)	9.9 ±0.1 (10.1)

[a] measured under an absolute irradiance (Power input) of 568 µW/cm2
[b] measured under an absolute irradiance (Power input) of 610 µW/cm2
[*] values are a calculated average over 8 or more devices
[**] device architecture used: glass/ITO/ZnO/(PDICA, for "Interlayer")/Active Layer BHJ/MoO_x/Ag
[***] solutions contain 1% (v/v) DPE additive
[****]values in brackets represent the best device

Table S7. OPV parameters of devices with PTQ10:tPDI$_2$N-EH active layers processed from toluene under various LED illumination conditions.

	Light Intensity (lux)	P_{in} (µW/cm^2)	V_{oc} (V)	J_{sc} (µA/cm^2)	FF %	PCE %
2700 K	ca. 400	113	0.97 ±0.01 (0.97)	20 ±1 (21)	50 ±3 (54)	8.5 ±0.7 (9.4)
	ca. 1000	288	1.00 ±0.01 (1.01)	57 ±6 (69)	45 ±1 (44)	8.9 ±0.8 (10.7)
	ca. 2000	568	1.05 ±0.02 (1.08)	106 ±3 (106)	50 ±4 (58)	9.8 ±1.0 (11.8)
6500 K	ca. 400	120	0.99 ±0.01 (0.99)	27 ±1 (27)	42 ±3 (45)	9.3 ±0.7 (10.3)
	ca. 1000	294	1.03 ±0.01 (1.02)	59 ±1 (60)	44 ±4 (49)	9.0 ±0.9 (10.2)
	ca. 2000	610	1.05 ±0.01 (1.06)	120 ±3 (119)	46 ±3 (53)	9.4 ±0.7 (10.9)

[*] values are a calculated average over 8 or more devices
[**] device architecture used: glass/ITO/ZnO/Active Layer BHJ/MoO_x/Ag
[***] solutions contain 1% (v/v) DPE additive
[****]values in brackets represent the best device

Table S8. OPV parameters of devices with PTQ10:tPDI$_2$N-EH active layers processed from toluene cast on top of ITO/ZnO/PDICA under various LED illumination conditions.

	Light Intensity (lux)	P_{in} (µW/cm^2)	V_{oc} (V)			J_{sc} (µA/cm^2)			FF %			PCE %		
2700 K	ca. 400	113	1.01	±0.01	(1.01)	22	±0	(22)	54	±2	(57)	10.5	±0.4	(11.1)
	ca. 1000	288	1.05	±0.00	(1.05)	53	±2	(58)	46	±1	(45)	8.9	±0.3	(9.6)
	ca. 2000	568	1.09	±0.01	(1.10)	112	±3	(116)	51	±4	(58)	10.9	±1.1	(12.9)
6500 K	ca. 400	120	1.01	±0.00	(1.01)	24	±0	(24)	50	±3	(56)	9.9	±0.7	(11.1)
	ca. 1000	294	1.04	±0.01	(1.03)	62	±1	(62)	48	±2	(52)	10.4	±0.3	(11.3)
	ca. 2000	610	1.07	±0.01	(1.06)	139	±9	(152)	48	±3	(47)	11.7	±0.4	(12.4)

* values are a calculated average over 8 or more devices
** device architecture used: glass/ITO/ZnO/Active Layer BHJ/MoO_x/Ag
*** solutions contain 1% (v/v) DPE additive
****values in brackets represent the best device

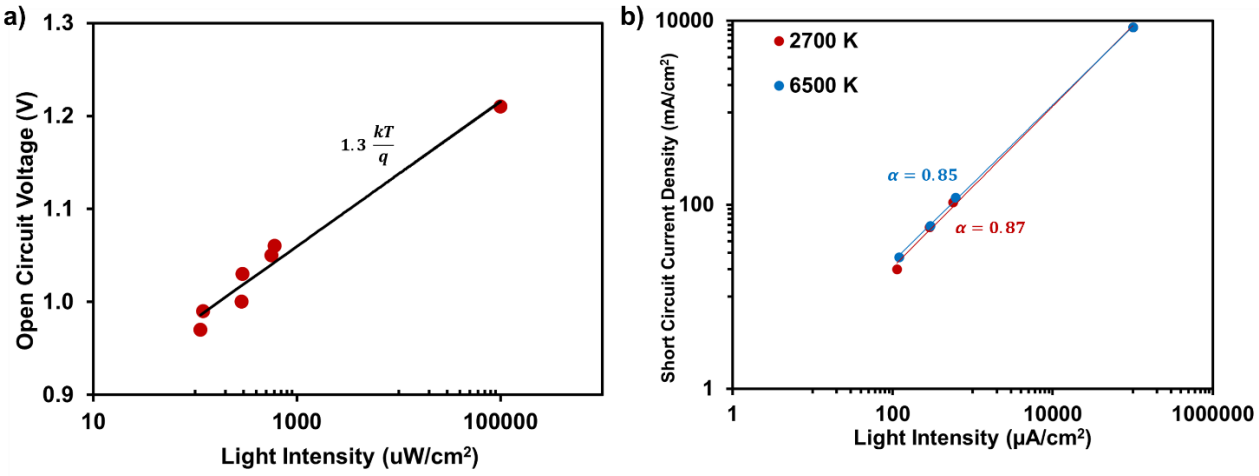

Figure S11. a) Measured V_{oc} of PTQ10:tPDI$_2$N-EH OPV devices as a function of illumination intensity; the value of the slope is 1.3 kT/q, which is indicative of the presence of monomolecular recombination at V_{oc} . b) Measured J_{sc} of PTQ10:tPDI2N-EH OPV devices as a function of illumination intensity (the one sun measurement was added to both 2700 K and 6500 K data sets), the value $\boldsymbol{\alpha}$ indicates the slope of the linear fit Jsc = (Light Intensity)$^{\alpha}$. These values of 0.85 and 0.87 indicate the presence of a moderate amount of bimolecular recombination occurring at J_{sc}.

PDI-EDOT-PDI Synthesis and Characterization

The synthesis of ethylhexyl N-annulated perylene diimide bromide (EH-NPDI-Br) was prepared according to known literature.[1]

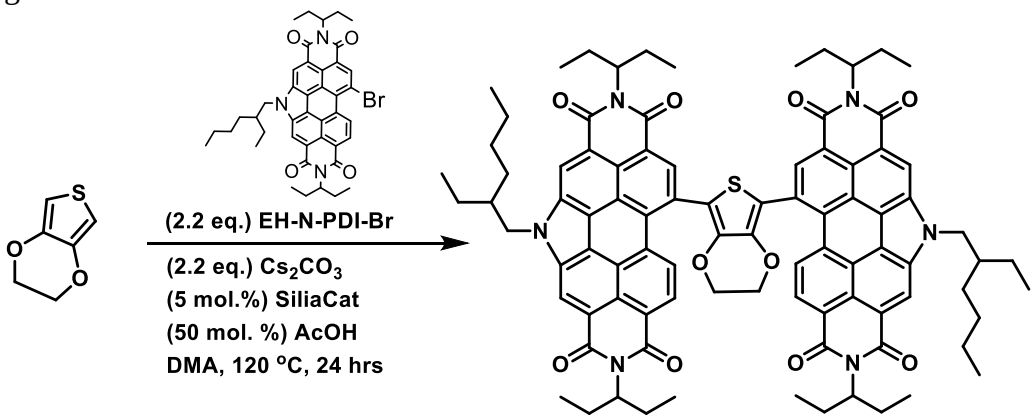

Into a 10 mL glass pressue vial, EH-N-PDI-Br (368 mg, 0.5 mmol, 2.2 eq.), Cs_2CO_3 (163 mg, 0.5 mmol, 2.2 eq.), SiliaCat-DPP (40 mg, 0.01 mmol, 5 mol.%) and EDOT (32.4 mg, 0.23 mmol, 1 eq.) were added. The vial was sealed and purged with N_2 for 30 mins. Dried DMA was Cannula transferred into the vial and then N_2 purged for 15 mins thereafter. Next, acetic acid (0.11 mmol, 50 mol.%) was injected and the reaction was placed into a 120 ºC bead bath and vigorously stir. When all starting material was consumed (monitoring by TLC), reaction was quenched by diluting with CH_2Cl_2 (~50mL) and then pouring through Celite plug to remove solids. All organic solvent was removed under reduced pressure. The crude product was purified by silica-gel column chromatography (eluted with CH_2Cl_2) and then collected by vacuum filtration, precipitating from methanol (311 mg, 0.21 mmol, 93%). The isolated compound matched previously reported spectroscopic properties.[10]

^{1}H NMR (500 MHz, Chloroform-*d*) δ 9.20 – 8.75 (m, *J* = 7.1 Hz, 10H), 5.26 (dtt, *J* = 12.9, 9.4, 5.7 Hz, 4H), 4.83 (h, *J* = 8.0, 7.4 Hz, 4H), 4.19 (s, 4H), 2.49 – 2.33 (m, 10H), 2.10 – 1.95 (m, 8H), 1.59 – 1.35 (m, 12H), 1.33 – 1.25 (m, 4H), 1.09 – 0.92 (m, 30H), 0.88 (t, *J* = 7.3 Hz, 6H).

^{13}C NMR (126 MHz, $CDCl_3$) δ 166.15, 164.83, 163.65, 138.61, 134.89, 134.75, 133.06, 132.37, 131.38, 129.73, 127.47, 126.79, 126.53, 124.29, 124.10, 122.72, 122.39, 121.83, 121.34, 119.32, 119.27, 118.50, 117.84, 116.93, 64.36, 57.30, 57.17, 50.40, 41.07, 30.34, 28.06, 24.69, 23.78, 22.49, 13.44, 10.90, 10.89, 10.18.

HRMS ($[M+Na]^+$) calculated for M = $C_{90}H_{92}N_6O_{10}S$: 1471.6488; detected $[M+Na]^+$: 1471.6423

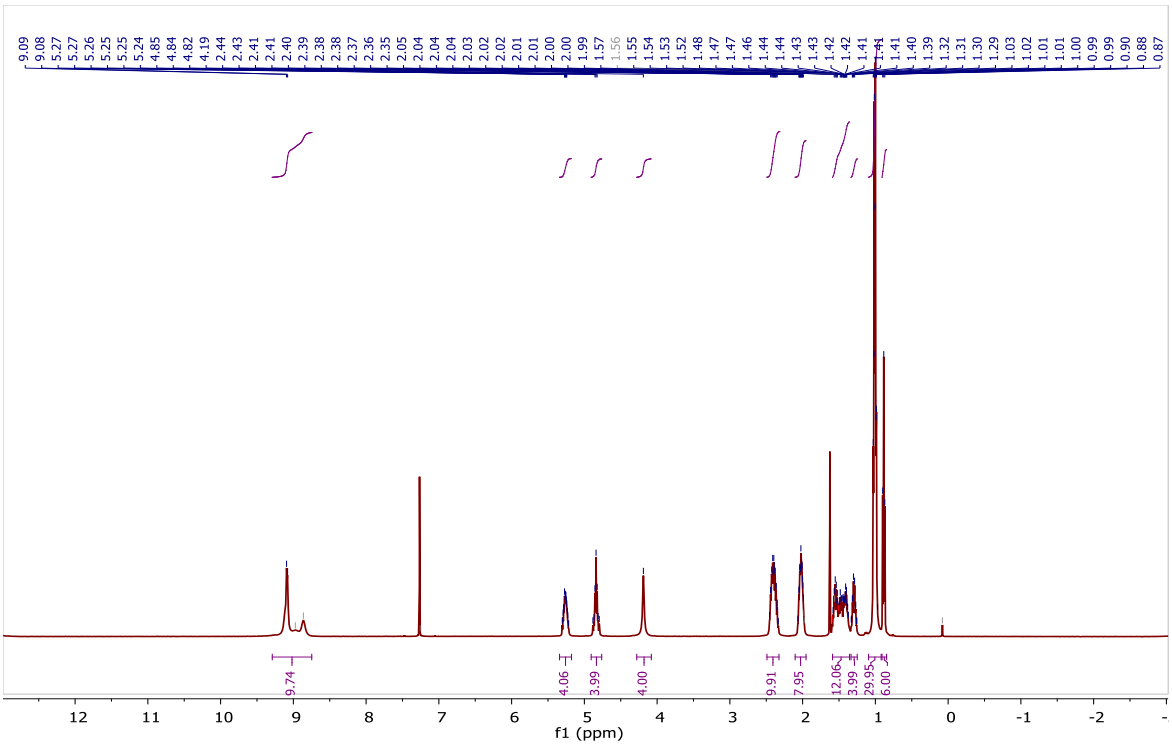

Figure S12. ^{1}H NMR spectrum of PDI-EDOT-PDI (500 MHz, $CDCl_3$, 295 K)

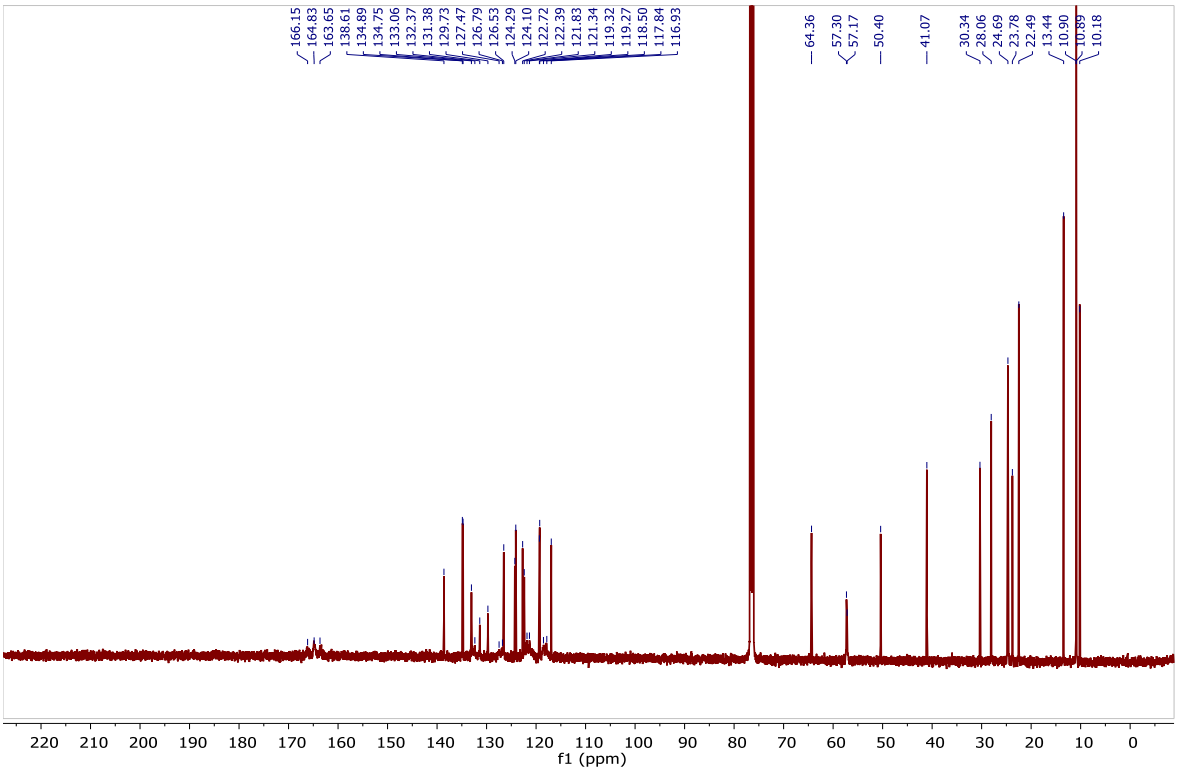

Figure S13. $^{13}C\{^{1}H\}$ NMR spectrum of PDI-EDOT-PDI (126 MHz, $CDCl_3$, 295 K)

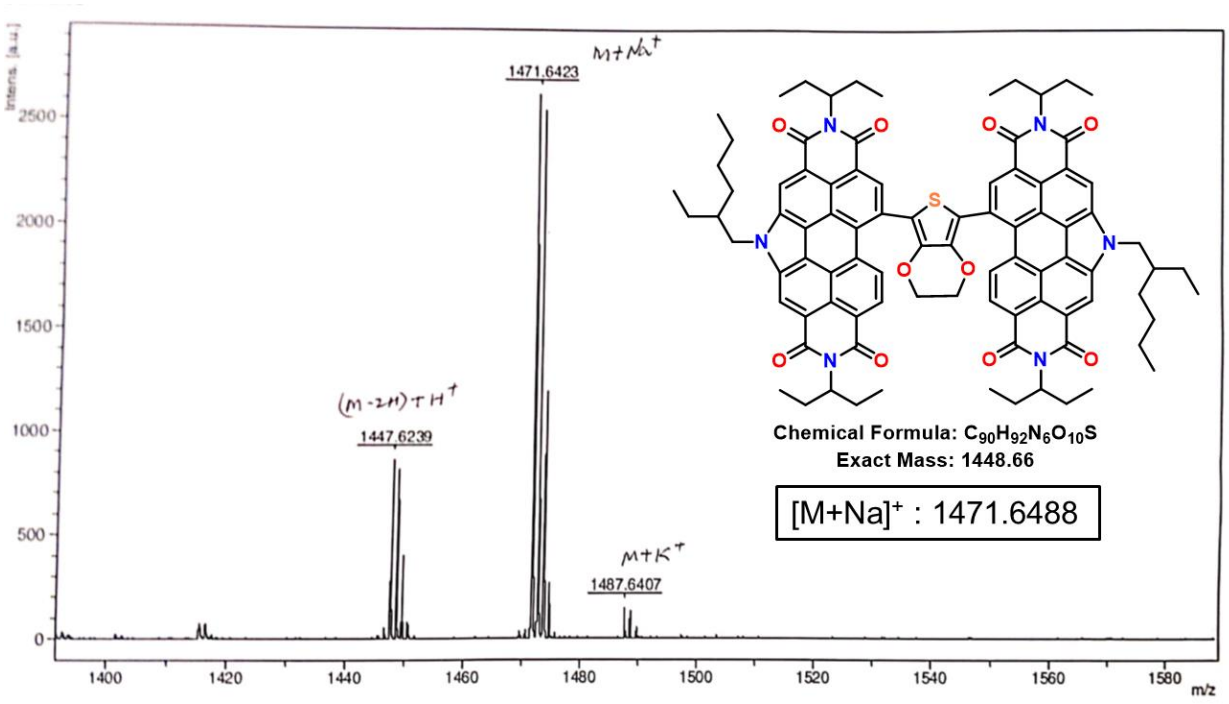

Figure S14. HR MALDI-TOF mass spectrum of PDI-EDOT-PDI.

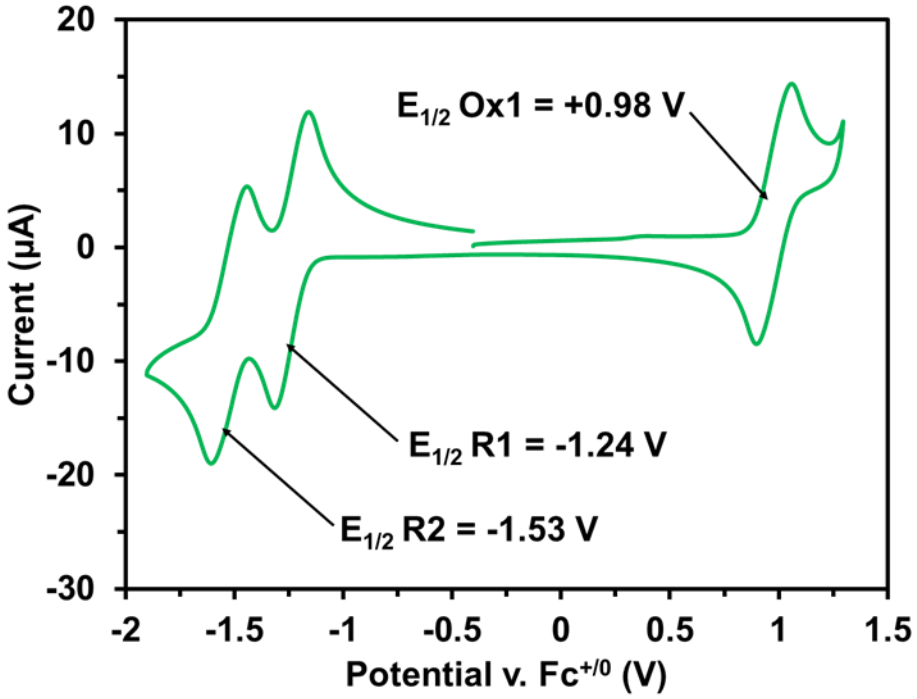

Figure S15. Cyclic voltammogram of PDI-EDOT-PDI recorded at 100 mV/s, under nitrogen in CH_2Cl_2 with 0.1 M $TBAPF_6$ as supporting electrolyte and $Fc^{+/0}$ as internal reference.

REFERENCES

(1) Dayneko, S. V.; Hendsbee, A. D.; Welch, G. C. Combining Facile Synthetic Methods with Greener Processing for Efficient Polymer-Perylene Diimide Based Organic Solar Cells. *Small Methods* **2018**, 1800081.

(2) Sun, Y.; Seo, J. H.; Takacs, C. J.; Seifter, J.; Heeger, A. J. Inverted Polymer Solar Cells Integrated with a Low-Temperature-Annealed Sol-Gel-Derived ZnO Film as an Electron Transport Layer. *Adv. Mater.* **2011**, *23* (14), 1679–1683.

(3) Pommerehne, J.; Vestweber, H.; Guss, W.; Mahrt, R. F.; Bässler, H.; Porsch, M.; Daub, J. Efficient Two Layer Leds on a Polymer Blend Basis. *Adv. Mater.* **1995**, *7* (6), 551–554.

(4) Schmidt, H.; Zilberberg, K.; Schmale, S.; Flügge, H.; Riedl, T.; Kowalsky, W. Transient Characteristics of Inverted Polymer Solar Cells Using Titaniumoxide Interlayers. *Appl. Phys. Lett.* **2010**, *96* (24), 243305.

(5) Kim, C. S.; Lee, S. S.; Gomez, E. D.; Kim, J. B.; Loo, Y.-L. Transient Photovoltaic Behavior of Air-Stable, Inverted Organic Solar Cells with Solution-Processed Electron Transport Layer. *Appl. Phys. Lett.* **2009**, *94* (11), 113302.

(6) Kim, J.; Kim, G.; Choi, Y.; Lee, J.; Heum Park, S.; Lee, K. Light-Soaking Issue in Polymer Solar Cells: Photoinduced Energy Level Alignment at the Sol-Gel Processed Metal Oxide and Indium Tin Oxide Interface. *J. Appl. Phys.* **2012**, *111* (11), 114511.

(7) Steim, R.; Choulis, S. A.; Schilinsky, P.; Brabec, C. J. Interface Modification for Highly Efficient Organic Photovoltaics. *Appl. Phys. Lett.* **2008**, *92* (9), 093303.

(8) Gilot, J.; Wienk, M. M.; Janssen, R. A. J. Double and Triple Junction Polymer Solar Cells Processed from Solution. *Appl. Phys. Lett.* **2007**, *90* (14), 143512.

(9) Forrest, S. R.; Bradley, D. D. C.; Thompson, M. E. Measuring the Efficiency of Organic Light-Emitting Devices. *Adv. Mater.* **2003**, *15* (13), 1043–1048.

(10) You, F.; Zhou, X.; Huang, H.; Liu, Y.; Liu, S.; Shao, J.; Zhao, B.; Qin, T.; Huang, W. *N* -Annulated Perylene Diimide Derivatives as Non-Fullerene Acceptors for Solution-Processed Solar Cells with an Open-Circuit Voltage of up to 1.14 V. *New J. Chem.* **2018**, *42* (18), 15079–15087.